

Cytopathology of liver and kidney in rainbow trout *Oncorhynchus mykiss* after long-term exposure to sublethal concentrations of linuron

Yasmina Oulmi¹, Rolf-Dieter Negele², Thomas Braunbeck^{1,*}

¹ Department of Zoology I, University of Heidelberg, Im Neuenheimer Feld 230, D-69120 Heidelberg, Germany

² Bavarian State Agency for Water Research, Experimental Station Wielenbach, Demollstraße, D-82407 Wielenbach, Germany

ABSTRACT: Hepatic and renal cytopathological alterations in fingerling rainbow trout *Oncorhynchus mykiss* following 5 wk exposure to 30, 120, and 240 $\mu\text{g l}^{-1}$ linuron [3(3,4-dichlorophenyl)-1-methoxy-1-methylurea] were studied by electron microscopy. Ultrastructural alterations were detected in liver and kidney at $\geq 30 \mu\text{g l}^{-1}$, 2 orders of magnitude below conventional LC_{50} . The response suggested a dose-response relationship with a change from adaptive to degenerative features at 120 $\mu\text{g l}^{-1}$. Hepatocyte changes included: stimulation of mitosis; segmentation of nuclei; partial reorganization of heterochromatin; multiplication of nucleoli; fractionation, vesiculation and transformation of rough endoplasmic reticulum (RER) into myelinated bodies; induction of smooth endoplasmic reticulum; moderate steatosis; apparent proliferation of mitochondria, peroxisomes, Golgi fields and lysosomal elements; depletion of glycogen; perisinusoidal lipid accumulation; elevated rate of hepatocytes in various stages of necrosis; infiltration and increased phagocytic activity of macrophages. Reactions of renal tubular cells were differentiated in different nephron segments. Major alterations by site in kidney were (1) renal corpuscle: lobulation of podocyte nuclei; (2) proximal segment I: elevated heterogeneity of all cell components, increased heterochromatin and nuclear size, rearrangement of RER, proliferation of Golgi fields, novel lysosomal elements, decreased mitochondria and lysosomes at 240 $\mu\text{g l}^{-1}$; (3) proximal segment II: nuclear lobulation, binucleated cells, proliferation of lysosomes and peroxisomes (lower concentrations), decreased peroxisomes and mitochondria (240 $\mu\text{g l}^{-1}$), crystalline inclusions in lysosomal matrix, fragmentation, degranulation and circular arrangement of RER; (4) distal segment: induction of giant mitochondria with longitudinal crystalline inclusions, atypical lysosomes with long crystalline matrix inclusions, and augmentation of various lysosomal elements. Comparison of linuron-induced cellular alterations with cytopathological effects by potential linuron breakdown products, namely 4-chloroaniline and 3,4-dichloroaniline, revealed a high degree of similarity of cytopathological phenomena, indicating that part of the changes observed after linuron exposure might well be due to the action of linuron metabolites.

KEY WORDS: Rainbow trout · Liver · Kidney · Ultrastructure · Linuron · 4-Chloroaniline · 3,4-Dichloroaniline · Cytopathology

INTRODUCTION

Due to its central role in metabolism and its proven sensitivity to environmental pollutants, the liver has been given particular attention in toxicological investigations on lethal and sublethal effects of organic and inorganic chemicals in both mammals and fish (Wester & Canton 1986, Phillips et al. 1987, Braunbeck 1994). A

series of communications demonstrated the plasticity of fish hepatocyte ultrastructure after exposure to environmentally relevant concentrations of organic xenobiotics in zebrafish *Brachydanio rerio* (Braunbeck et al. 1989, 1990a, b, 1992a), rainbow trout *Oncorhynchus mykiss* (Braunbeck et al. 1990b, Braunbeck 1994), eel *Anguilla anguilla* (Braunbeck & Völkl 1991, Arnold & Braunbeck 1994), golden ide *Leuciscus idus melanotus* (Braunbeck & Völkl 1993), and medaka *Oryzias latipes* (Braunbeck et al. 1992b) as well as in isolated hepato-

* Addressee for correspondence

cytes from rainbow trout liver (Braunbeck 1993, Zahn & Braunbeck 1993, Zahn et al. 1993). In contrast to the liver, fish kidney has only rarely been studied with regard to cytological alterations induced by xenobiotic compounds (Rojik et al. 1983, Benedeczy et al. 1986, Reimschuessel et al. 1989, Fischer-Scherl et al. 1991). Since most environmental contamination occurs at low to very low concentrations, highly sensitive methods have to be applied in order to elucidate not only acute toxic effects, but also sublethal reactions of organisms. For this purpose, electron microscopy has been shown to be a method of choice (Braunbeck 1994).

Linuron was chosen as a model substance, since urea derivatives have not so far been studied with respect to cytological effects in fish. In 1960, linuron was the first urea-type herbicide to be commercialized as a herbicide. The potential of linuron to accumulate in aquatic and terrestrial systems is comparatively low (Kempson-Jones & Hanel 1979, Zahnow & Riggelman 1980, Maier-Bode & Hartel 1981). Although there is only limited risk of bioaccumulation in mammals (Hodge et al. 1968), with highest values in faeces and urine as well as in adipose tissues and the liver (Maier-Bode & Hartel 1981), linuron was included in a list of 129 chemicals to be given priority in future investigations (Malle 1984). Whereas in older reports the mutagenic and carcinogenic potential of linuron appeared ambiguous (Hodge et al. 1968, Fishbein 1972, Marshall et al. 1976, Worthing 1987), the US Academy of Sciences recently registered linuron in a list of 28 pesticides considered as potential carcinogens (Roloff et al. 1992). With regard to both toxicity and carcinogenic risk of linuron, contamination by parent and breakdown compounds such as 3,4-dichloroaniline, 4-chloroaniline and hydroxylated derivatives (Maier-Bode & Hartel 1981, Lewalter & Korallus 1986) must be taken into consideration. With respect to the evaluation of environmental risk, 3,4-dichloroaniline and 4-chloroaniline could be documented in the Rhine and Meuse rivers at concentrations up to $1.5 \mu\text{g l}^{-1}$ (Greve & Wegman 1975, Herzel & Schmidt 1977). Only recently, aromatic chlorinated amines in fish were shown to be transformed by N-hydroxylation to nitrosoarene compounds via nitroso compounds and hydroxylamine (Dady et al. 1991), and the carcinogenic potential of chloroanilines in fish has been demonstrated for medaka *Oryzias latipes* (Johnson & Teitge 1991). As in any 3,4-dichloroaniline derivative, tetrachloroazobenzene and tetrachloroazoxybenzene can be present as further contaminants of linuron (Sundström et al. 1978, Hill et al. 1981, Di Muccio et al. 1984). These compounds are isosteric to tetrachlorodibenzo-*p*-dioxin (TCDD) and tetrachlorodibenzofuran (TCDF), 2 of the most potent toxins and teratogens known (Hsia et al. 1977, Scharinkel et al.

1980, 1982), and, at least in mammals, their toxicities are comparable to that of TCDD and TCDF.

The acute toxicity of linuron to fish (LC_{50}) ranges from 0.6 to 3.5 mg l^{-1} in harlequin fish *Rasbora heteromorphia* (Tooby et al. 1975) to $>20 \text{ mg l}^{-1}$ in carp *Cyprinus carpio* (Knauf & Schulze 1972). According to Knauf & Schulze (1972), LC_{0} and LC_{100} data for rainbow trout are 5 and 10 mg l^{-1} , respectively, and Worthing (1987) gives an LC_{50} value of 16 mg l^{-1} for this species. Except for one report on inhibition of phagocytosis activity in rainbow trout leucocytes at a concentration of $30 \mu\text{g l}^{-1}$ (Falk et al. 1990), no data are available on sublethal effects of linuron in fish.

MATERIALS AND METHODS

Fish culture and maintenance. Rainbow trout were reared from embryonated eggs under constant aeration in large-scale flow-through systems at the field station of the Bavarian Federal Agency for Water Research, Wielenbach, Germany. The quality of the well water was maintained at $379 \text{ mg l}^{-1} \text{ CaCO}_3$ (21.3°dH hardness), $744 \mu\text{S}$ (conductivity), $\text{pH } 7.66 \pm 0.1$, $10.5 \pm 0.5 \text{ mg l}^{-1} \text{ O}_2$ and $9.4 \pm 0.5^\circ \text{C}$ throughout the rearing and experimental periods. Ammonia, nitrite and nitrate were kept below detection limits. During the experiment, duplicate groups of 10 individuals with a weight of $14.1 \pm 2.3 \text{ g}$ and a length of $10.0 \pm 1.8 \text{ cm}$ for each linuron concentration were kept in a permanent flow-through system with 36 l full glass-aquaria and a water exchange rate of 2 l h^{-1} . Prior to use, water was prefiltered with activated charcoal (Aquapur™, Thyssen, Germany) to eliminate potential impurities. Fish were fed with commercially available trout chow (Trouvit™ bio 100) at a daily rate of 1% body weight throughout the experiment. Dietary components were 47% protein (3% lysine), 1.5% fibrous material, 12% lipid, and 8% ash. Faeces and excess food particles were removed twice daily; aquaria screens were cleaned daily. Photoperiod was 12 h light and 12 h dark.

Linuron exposure and analytical procedures. Exposure time was 5 wk. 75 mg linuron [3(3,4-dichlorophenyl)-1-methoxy-1-methylurea] of 99.96% purity (lot number 870318; Ehrenstorfer GmbH, Augsburg, Germany) were dissolved in 1 l of distilled water by stirring for 24 h at 20°C , quickly heated under pressure, cooled to 10°C and passed through $0.2 \mu\text{m}$ membrane filters. Stock solutions were stored in light-proof bottles. The amount of toxicant in the aquaria was adjusted to 0, 30, 120 and $240 \mu\text{g l}^{-1}$ linuron by continuously adding stock solution to the water input by means of precision peristaltic pumps (Minipuls™, Gilson); water input was controlled by flowmeters (rotameter™, Rota Yokogawa,

Wehr, Germany). Linuron concentrations in aquaria were determined once weekly by means of HPLC with UV detection after solid-phase extraction with RC-C18-carrier and organic solvent elution. Actual linuron values for nominal concentrations of 0, 30, 120 and 240 $\mu\text{g l}^{-1}$ were 0, 30.8 ± 6.2 , 125.8 ± 17.3 , and $235.8 \pm 10.4 \mu\text{g l}^{-1}$, respectively. Wastes were purified by passing through active charcoal.

Electron microscopy. To control for diurnal variation, all sampling was performed during midmorning. Livers and kidneys of 4 fish from control and treated groups were collected and anaesthetized in 4-amino benzoic acid ethyl ester (benzocaine; 50 mg l^{-1}). *In situ* cardiac perfusion fixation was achieved through the ventricular wall using a Reglo-MS 8TM peristaltic pump (Ismatec, Zürich, Switzerland) equipped with a 2.5 mm I.D. TygonTM tube (Ismatec) and a blunt 0.9 mm steel needle with a terminal opening of 0.6 to 0.7 mm (MicrolanceTM, Becton & Dickinson, Dublin, Ireland). The vasculature was flushed with 4°C fish physiological saline containing 2% polyvinylpyrrolidone (PVP, Merck, Darmstadt, Germany) and 0.5% procainhydrochloride (Merck) for 30 s to remove blood cells. This was followed by 1.5% glutardialdehyde and 1.5% formaldehyde (freshly prepared from paraformaldehyde) in 0.1 M sodium phosphate buffer (pH 7.6) containing 2.5% PVP (4°C). Initial perfusion rate was adjusted to between 5 and 6 ml min^{-1} . Livers were excised immediately after perfusion, immersed in perfusion fixative for 20 min, and cut into slices of 60 to 70 μm using an Oxford vibratome. Kidney samples were dissected, cut into small cubes of 500 μm side length, and immersed in perfusion fixative for at least 60 min. Fixation was continued in 2.5% glutardialdehyde in 0.1 M sodium cacodylate buffer (pH 7.6) containing 4% PVP and 0.05% calcium chloride for 20 min. After rinsing in cacodylate buffer, tissue slices were postfixed for 1 h with 1% osmium ferrocyanide (Karnovsky 1971). After washing in 0.1 M cacodylate and 0.05 M maleate buffer (pH 5.2), tissues were stained en bloc with 1% uranyl acetate in maleate buffer for 1 h. Specimens were dehydrated in a graded series of ethanol and embedded in Spurr's medium (Spurr 1969). Ultrathin sections of 60 to 80 nm thickness were stained with alkaline lead citrate (Reynolds 1963) for 30 s or 1 min and examined in a Zeiss EM 9 or EM 10 electron microscope.

Light microscopy. Semithin plastic sections of 0.5 μm were stained with methylene blue-Azur II (Richardson et al. 1960; modified) and used only for orientation. For visualization of glycogen, semithin sections were incubated in an alkaline 1% solution of silver diamine for 1.5 h at 60°C (Singh 1964). After rinsing in distilled water, sections were mounted in Entellan and examined in a Leitz Aristoplan photomicroscope.

RESULTS

Liver alterations

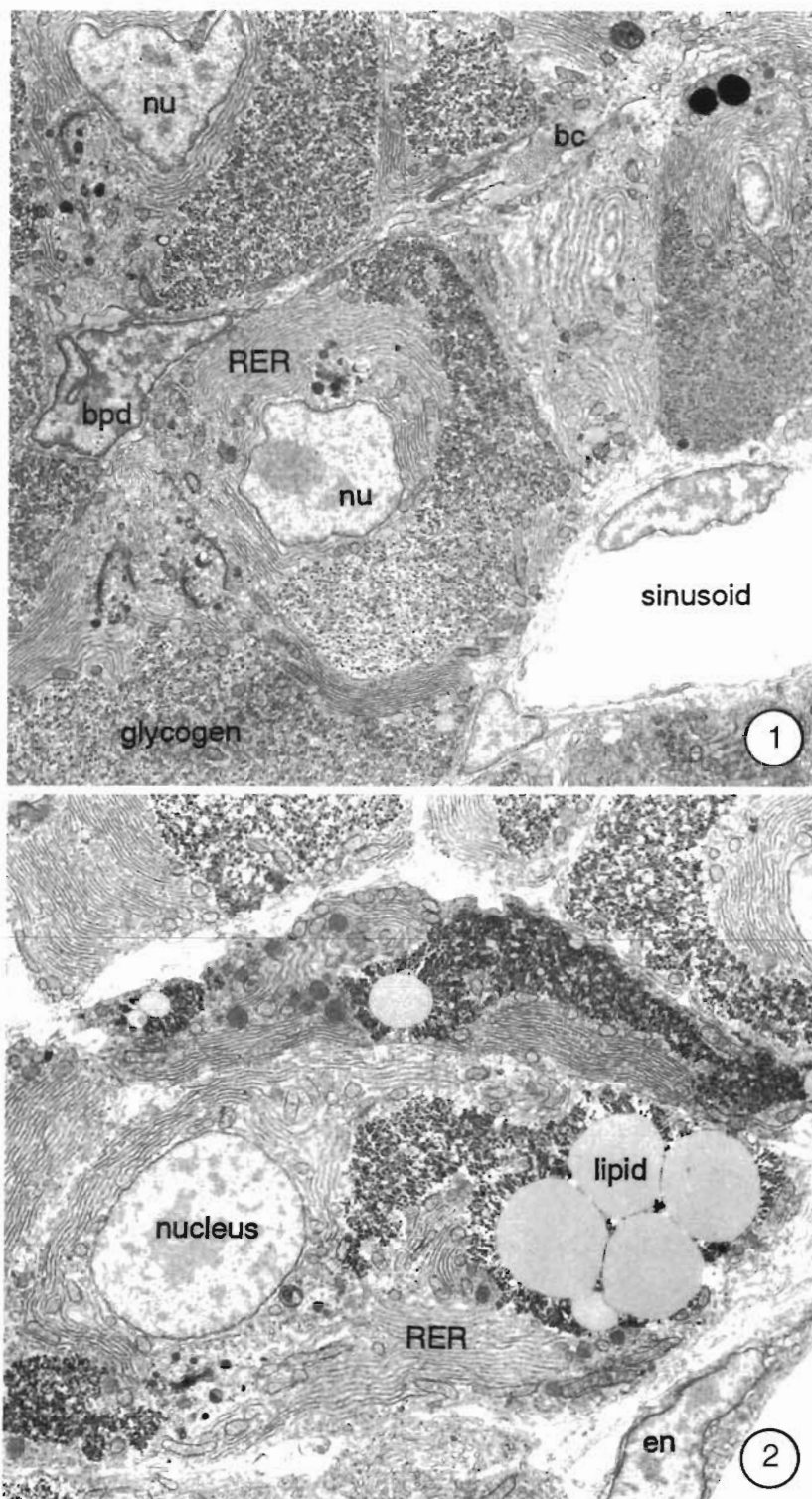
Controls

Since the ultrastructure of rainbow trout liver has been described in detail several times (Scarpelli et al. 1963, Berlin & Dean 1967, Hacking et al. 1978, Chapman 1981, Hampton et al. 1985, 1988, 1989, Braunbeck et al. 1990b, Braunbeck 1994), only a brief outline of control liver ultrastructure will be given. Hepatocytes are typical epithelial cells with a size range from 15 to 25 μm characterized by distinct polarity, with the apical pole facing the biliary system and the basal pole located vis-à-vis the endothelial lining of sinusoids (Fig. 1). Cells are regularly arranged in tubules with 3 to 5 hepatocytes contributing to form the central bile canaliculus ('tubular liver architecture'; Hampton et al. 1985, 1988) and characterized by a conspicuous separation into extended peripheral glycogen fields with few lipid inclusions and perinuclear organelle-containing portions of cytoplasm ('intracellular compartmentation'; Braunbeck et al. 1990b). Extensive stacks of rough endoplasmic reticulum (RER) cisternae interspersed with few mitochondria form an almost continuous sheath around the centrally located nucleus. In contrast, smooth endoplasmic reticulum (SER) is restricted to minute peribiliary areas. The ovoid nucleus bears little randomly scattered heterochromatin and a distinct nucleolus. RER stacks are separated from glycogen fields by large amounts of spherical coreless peroxisomes. Between the nucleus and the bile canaliculus, the RER sheath is interrupted by the peribiliary area comprising Golgi fields of several piles of 3 to 5 cisternae budding off numerous vesicles with abundant VLDL (Very Low Density Lipoprotein) granules and lysosomal elements.

Rainbow trout exposed to linuron

Following exposure to 30 $\mu\text{g l}^{-1}$ linuron, basic microscopical features of liver parenchyma and intracellular compartmentation of hepatocytes appeared unaltered. Hepatocellular alterations, although present, were not consistent in all individuals. All modifications described for 30 $\mu\text{g l}^{-1}$ were seen at higher concentrations. From a qualitative point of view, a distinction between hepatocytes of fish subjected to 120 $\mu\text{g l}^{-1}$ and specimens exposed to 240 $\mu\text{g l}^{-1}$ was not feasible; ultrastructural alterations, however, were more pronounced at the higher concentration, suggesting a dose-response relationship (Table 1).

At lower magnifications, modifications of hepatocytes included RER fractionation and an accumulation of lipid



Figs 1 & 2 *Oncorhynchus mykiss* Fig. 1. The cytoplasm of hepatocytes in control rainbow trout is characterized by a distinct separation into a central organelle-containing portion dominated by extensive stacks of long continuous cisternae of rough endoplasmic reticulum (RER) around the nucleus (nu) and into peripheral areas of glycogen deposits. bc: bile canaliculus; bpd: bile preductular cell $\times 4000$. Fig. 2. At low magnifications, hepatocytes of rainbow trout exposed to $\geq 120 \mu\text{g l}^{-1}$ linuron display progressive fragmentation of the RER cisternae as well as a conspicuous accumulation of lipid droplets in the perisinusoidal portion of the cells. en: endothelial lining of sinusoid $\times 3800$.

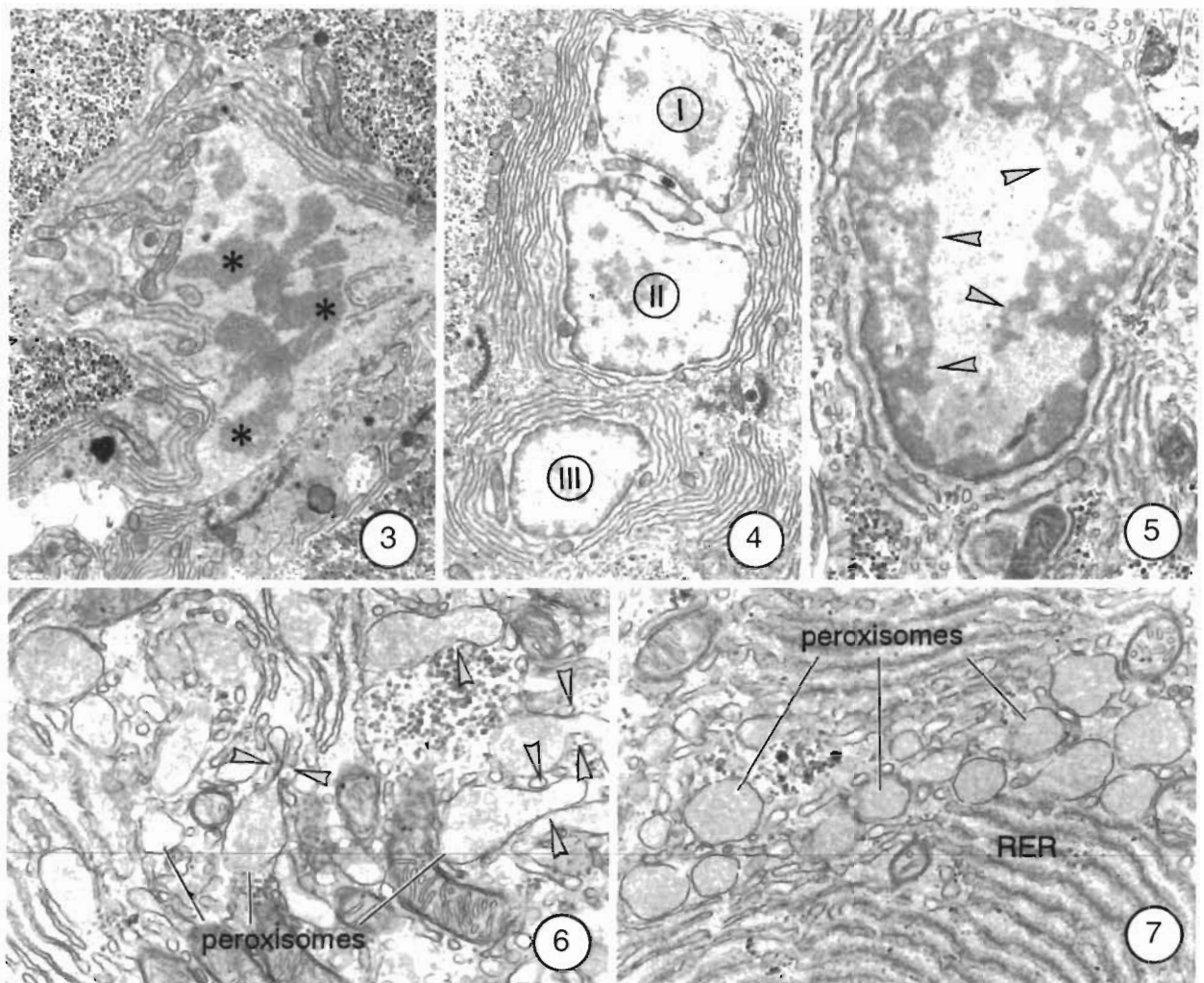
droplets at the perisinusoidal pole (Fig. 2). In contrast, with increasing linuron concentrations, progressive depletion in glycogen was observed. There was an apparent increase of hepatocellular mitosis after exposure to $30 \mu\text{g l}^{-1}$ (Fig. 3). Since the ratio of binucleated cells did not change, and macroscopically overt changes in the liver were not discerned, the increase in the number of hepatocytes was apparently compensated for by a decrease in cell size, partly explained by a decline in hepatocellular glycogen stores. Part of the hepatocyte nuclei displayed a slight expansion of heterochromatin fields, the nuclear outline was less regular, and, occasionally, deep cytoplasmic pseudoinvasions into the nuclei could be observed. In some individuals exposed to 120 or $240 \mu\text{g l}^{-1}$, nuclear heterogeneity led to an apparent segmentation of the nuclei (Fig. 4). Additional alterations within the nucleus were comprised of small non-membrane-bound intranuclear lipid inclusions, atypical web-like distribution of heterochromatin underneath the nuclear envelope (Fig. 5), and an increase in size and number of nucleoli.

Dilation of the intermembranous space in mitochondria and elevated morphological heterogeneity of peroxisomes were the sole mitochondrial and peroxisomal modifications after exposure to $30 \mu\text{g l}^{-1}$. In contrast, at $\geq 120 \mu\text{g l}^{-1}$, both organelles displayed a pronounced proliferation in conjunction with increased morphological heterogeneity. Mitochondria tended to transform to dumbbell-like shapes, while typical peroxisomal changes included formation of tail-like protrusions (Fig. 6) as well as accumulation into clusters and around cytoplasmic lipid inclusions (Figs. 6 & 7).

Two specimens at $30 \mu\text{g l}^{-1}$ displayed peribiliary accumulation of SER. RER lamellae, in close spatial relationship to lipid droplets (Fig. 8), were transformed into concentric arrays (Fig. 9). At $\geq 120 \mu\text{g l}^{-1}$, overall RER showed a slight but pro-

Table 1. *Oncorhynchus mykiss*. Cytological alterations in the liver of rainbow trout after prolonged sublethal exposure to various concentrations of linuron. –: absent; +: little developed; ++: moderately developed; +++: strongly developed; ++++: very strongly developed

	Controls	30 µg l ⁻¹	120 µg l ⁻¹	240 µg l ⁻¹
Organisation of liver parenchyma				
Interindividual variability of parenchyma	–	+	++	++
Disturbance of compartmentation	–	–	(+)	(+)
Single cell necrosis	–	(+)	++	+++
Nuclei				
Stimulation of mitosis	–	+	++	++
Free nuclear lipid inclusions	–	–	+	++
Atypical distribution of heterochromatin	–	–	++	+++
Deformation of nuclear envelope	–	+	+++	+++
Formation of pseudoinvaginations	–	+	+++	+++
Augmentation of nucleoli	–	–	++	+++
Size increase of nucleoli	–	–	+	++
Mitochondria				
Proliferation	–	–	++	+++
Increased heterogeneity	–	(+)	+	++
Dilation of intermembranous space	–	–	(+)	+
Peroxisomes				
Proliferation	–	–	++	+++
Increased heterogeneity	–	–	+	++
Cluster formation	–	(+)	+	++
Tail formation (division?)	–	(+)	+	++
Accumulation around lipid	–	–	(+)	(+)
Rough endoplasmic reticulum				
Increased heterogeneity	–	–	+	++
Reduction	–	–	(+)	+
Fragmentation, vesiculation	–	–	++	+++
Dilation of cisternae	–	–	+	+
Steatosis	–	–	+	+
Formation of RER whorls	–	+	++	++
Transformation into myelin body(ies)	–	–	+	+++
Smooth endoplasmic reticulum				
Proliferation	–	(+)	+	+
Golgi fields				
Increased heterogeneity	–	–	++	++
Hypertrophy	–	–	++	+++
Fenestration of cisternae	–	–	+	++
Stimulation of VLDL synthesis	–	(+)	++	++
Augmentation of Golgi vesicles	–	–	+	+
Lysosomal elements				
Proliferation	–	(+)	+	++
Induction of new lysosome types	–	(+)	+	++
Phospholipidosis	–	–	++	++
Myelinated bodies	–	(+)	+	++
Induction of autophagosomes	–	(+)	++	+++
Induction of multivesicular bodies	–	–	(+)	(+)
Induction of glycogenosomes	–	(+)	+	+
Storage materials				
Increase of lipid deposits	–	+	+++	++++
Perisinusoidal accumulation of lipids	–	+	+	++
Steatosis	–	–	+	+
Formation of lipid clusters	–	–	+	++
Free nuclear lipid inclusions	–	–	+	++
Decrease in glycogen stores	–	+	+++	++++
Induction of glycogenosomes	–	(+)	+	+
Non-parenchymal cells				
Immigration of macrophages	–	+	+++	+++
Formation of macrophage centres	–	–	+	++
Increased glycogen phagocytosis	–	–	++	+++



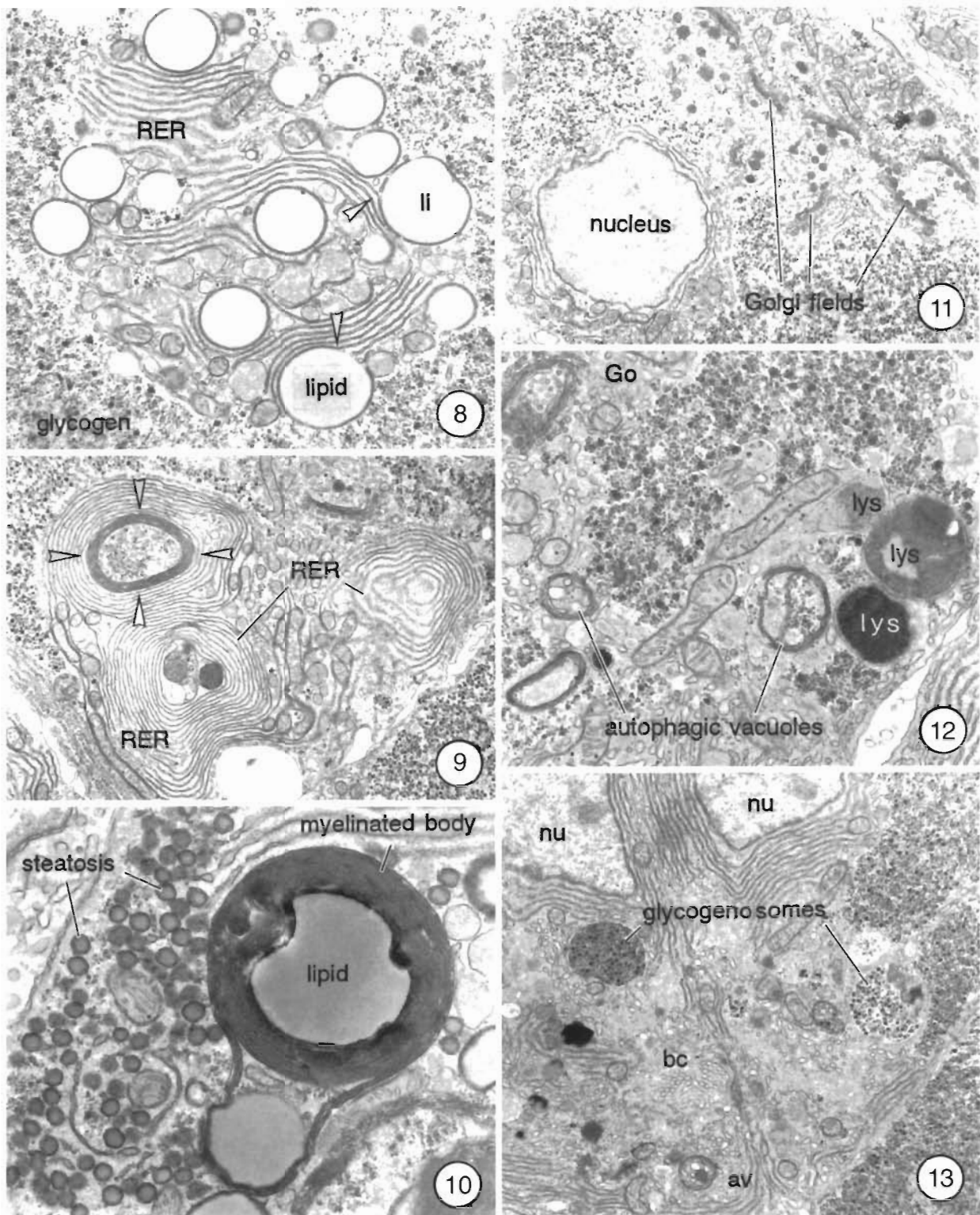
Figs 3 to 7 *Oncorhynchus mykiss*. Figs. 3 to 5. Hepatocellular nuclear changes induced by exposure to linuron include an increased rate of hepatocytes in mitosis ($\geq 30 \mu\text{g l}^{-1}$, Fig. 3, *) as well as the induction of segmented nuclei ($\geq 30 \mu\text{g l}^{-1}$; Fig. 4, I-III) and highly unusual heterochromatin distribution patterns ($\geq 120 \mu\text{g l}^{-1}$, Fig. 5 arrowheads). Figs. 6 & 7. Predominantly along the edges of the peripheral glycogen fields, hepatocytes of rainbow trout exposed to $\geq 120 \mu\text{g l}^{-1}$ linuron show a marked proliferation of peroxisomes in conjunction with a highly polymorphic outline of peroxisomal profiles (Fig. 6: arrowheads). Fig. 3: $\times 4300$; Fig. 4: $\times 5500$, Fig. 5: $\times 10000$, Fig. 6: $\times 22700$, Fig. 7: $\times 21300$

gressive decline. Single cisternae fractioned and vesiculated, and concentric stacks of cisternae condensed into myelin-like membrane whorls, usually with lipid droplets, but also other organelles, as centers (Figs. 9 & 10). Hepatocytes exposed to $240 \mu\text{g l}^{-1}$ displayed a proliferation of SER as an irregular network of undulating and anastomosing tubular or vesicular profiles. In some hepatocytes, accumulation of microvesicular lipid or lipoprotein granules within RER cisternae indicated onset of steatosis (Fig. 11).

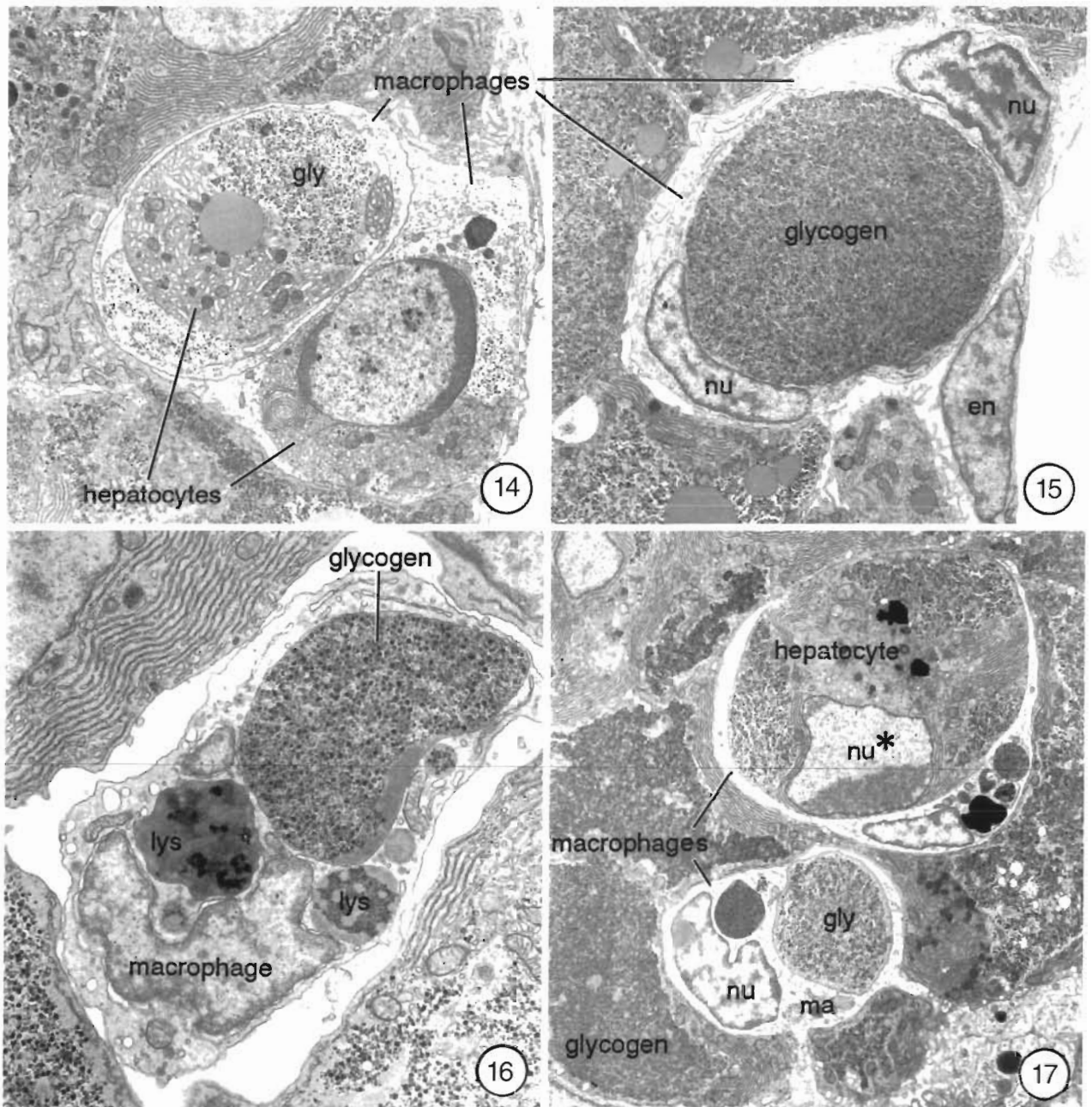
Whereas alterations in Golgi fields such as augmentation of dictyosomes with slightly fenestrated cisternae and increased numbers of Golgi vesicles only became apparent after exposure to $\geq 120 \mu\text{g l}^{-1}$, an augmentation of lysosomes, myelinated bodies, auto-

phagosomes and glycogenosomes was evident at $\geq 30 \mu\text{g l}^{-1}$ (Figs. 12 & 13). At $\geq 120 \mu\text{g l}^{-1}$, the lysosomal compartment not only showed pronounced proliferation, but also included multivesicular bodies and new types of secondary lysosomes with stacks of membranous material (phospholipidosis).

At $\geq 30 \mu\text{g l}^{-1}$ linuron, the number of hepatocytes in advanced stages of necrosis was increased. Most necrotic cells were ingested by macrophages (Figs. 14 to 17), which apparently invaded the liver parenchyma along the biliary tract and via the space of Disse. Macrophages, characterized by an irregularly shaped nucleus with appreciable amounts of heterochromatin, contained conspicuous lysosomal inclusions, occasionally reaching considerable dimensions (Figs. 16 & 17).



Figs. 8 to 13 *Oncorhynchus mykiss* Figs. 8 to 10 Following exposure to linuron, cisternae of the rough endoplasmic reticulum (RER) show a most intimate association with lipid (li) droplets ($\geq 30 \mu\text{g l}^{-1}$, Fig. 8, at arrowheads, note the approach of RER cisternae to surface of lipid droplets) and progressive transformation into concentric arrays ($\geq 30 \mu\text{g l}^{-1}$, Fig. 9 arrowheads) and — eventually — myelinated bodies ($\geq 120 \mu\text{g l}^{-1}$, Fig. 10). Moreover, lipid accumulation within small vesicles of endoplasmic reticulum indicates steatosis ($\geq 120 \mu\text{g l}^{-1}$, Fig. 10). Figs. 11 to 13 In the peribiliary fields of hepatocytes in rainbow trout subjected to $\geq 120 \mu\text{g l}^{-1}$ linuron, there is a pronounced increase in the number and the morphological heterogeneity of Golgi fields (Fig. 11) as well as a proliferation of lysosomes (lys), autophagic vacuoles (Figs. 12, 13 av) and glycogenosomes (Fig. 13) bc bile canaliculus Fig. 8. $\times 10900$, Fig. 9 $\times 7500$, Fig. 10 $\times 20500$, Fig. 11 $\times 6300$, Fig. 12 $\times 12500$, Fig. 13 $\times 6700$



Figs 14 to 17. *Oncorhynchus mykiss*. After exposure to $\geq 30 \mu\text{g l}^{-1}$ linuron, there was an increase in the number of necrotic hepatocytes ingested by macrophages (ma). Macrophages were characterized by an irregularly shaped nucleus (nu) containing appreciable amounts of heterochromatin and conspicuous lysosomal inclusions (lys) occasionally reaching considerable dimensions (Figs 16, 17). Apparently, macrophages accumulated vast amounts of glycogen (gly). nu*: nucleus of ingested hepatocyte. Fig 14: $\times 3800$, Fig 15: $\times 4700$, Fig 16: $\times 5900$, Fig 17: $\times 3900$.

Apparently, macrophages accumulated vast amounts of glycogen (most likely derived from hepatocytes) within vacuoles (Figs. 15 to 17). At $\geq 120 \mu\text{g l}^{-1}$, the rate of hepatocellular necrosis was drastically raised, and macrophages displayed further augmentation and tended to form conspicuous macrophage centers in

areas where apparent cell necrosis had resulted in free spaces within the parenchyma. Macrophages were no longer restricted to their routes of invasion, but were randomly scattered throughout the parenchyma. Biliary cells and endothelia were apparently free of cytopathological effects.

Kidney alterations

Controls

Investigations were restricted to epithelial cells of renal corpuscles and tubules. Segmentation of the rainbow trout nephron has been shown by Hentschel & Finkenstädt (1980) as well as Yasutake & Wales (1983), and terminology of tubular segments is based on the review by Hentschel & Elger (1987). Since there is appreciable heterogeneity in nephrons due to age and environmental conditions (Hentschel & Elger 1987), an outline of the ultrastructure of control kidneys is given.

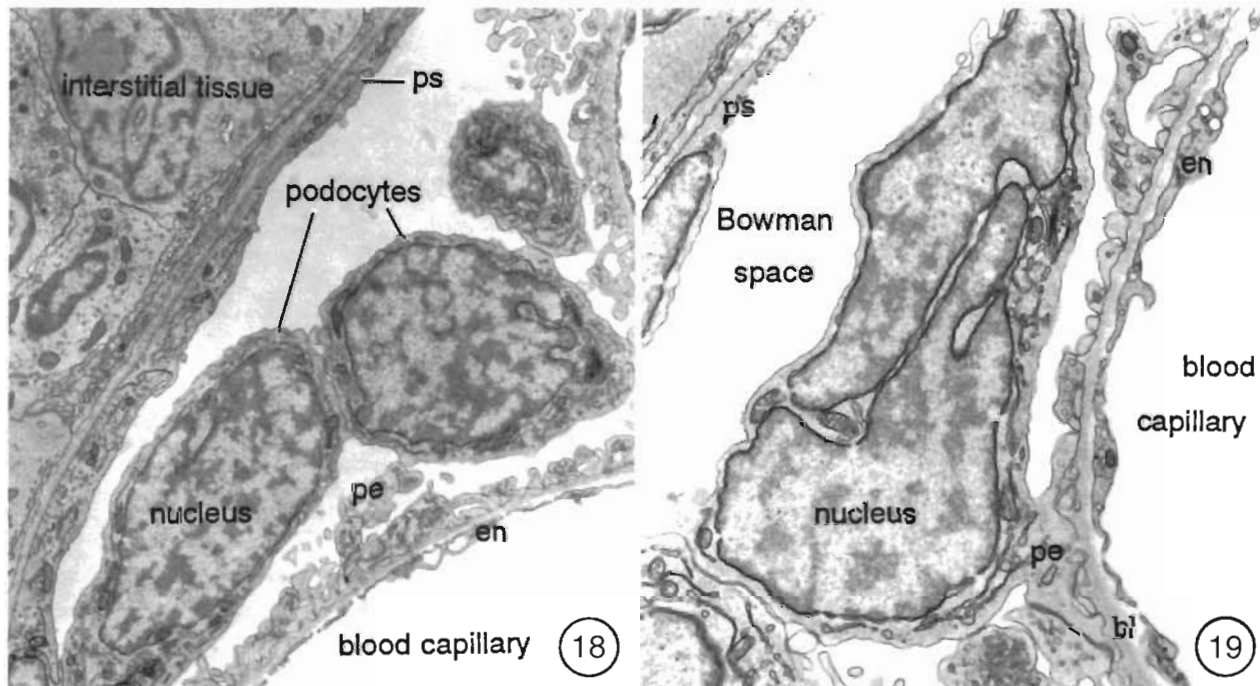
In renal corpuscles, podocytes show a round to slightly lobulated nucleus filling almost the entire cell and containing considerable heterochromatin (Fig. 18). Mitochondria are few and the endoplasmic reticulum (ER) system and Golgi fields are well developed. Pedicelles connected by a thin diaphragm are separated from the endothelial layers of the capillary loops by a basal lamina of 0.25 to 0.40 μm . The outer sheet of Bowman's capsule consists of extended cells with flattened nuclei and few organelles.

Proximal segments I (PS I) consist of columnar cells (12.9 to 17.2 μm) with a high brush border (2.3 to 3 μm) and a basally located nucleus containing little heterochromatin (see Fig. 20). Nuclear envelopes may appear slightly distended. Abundant microtubules,

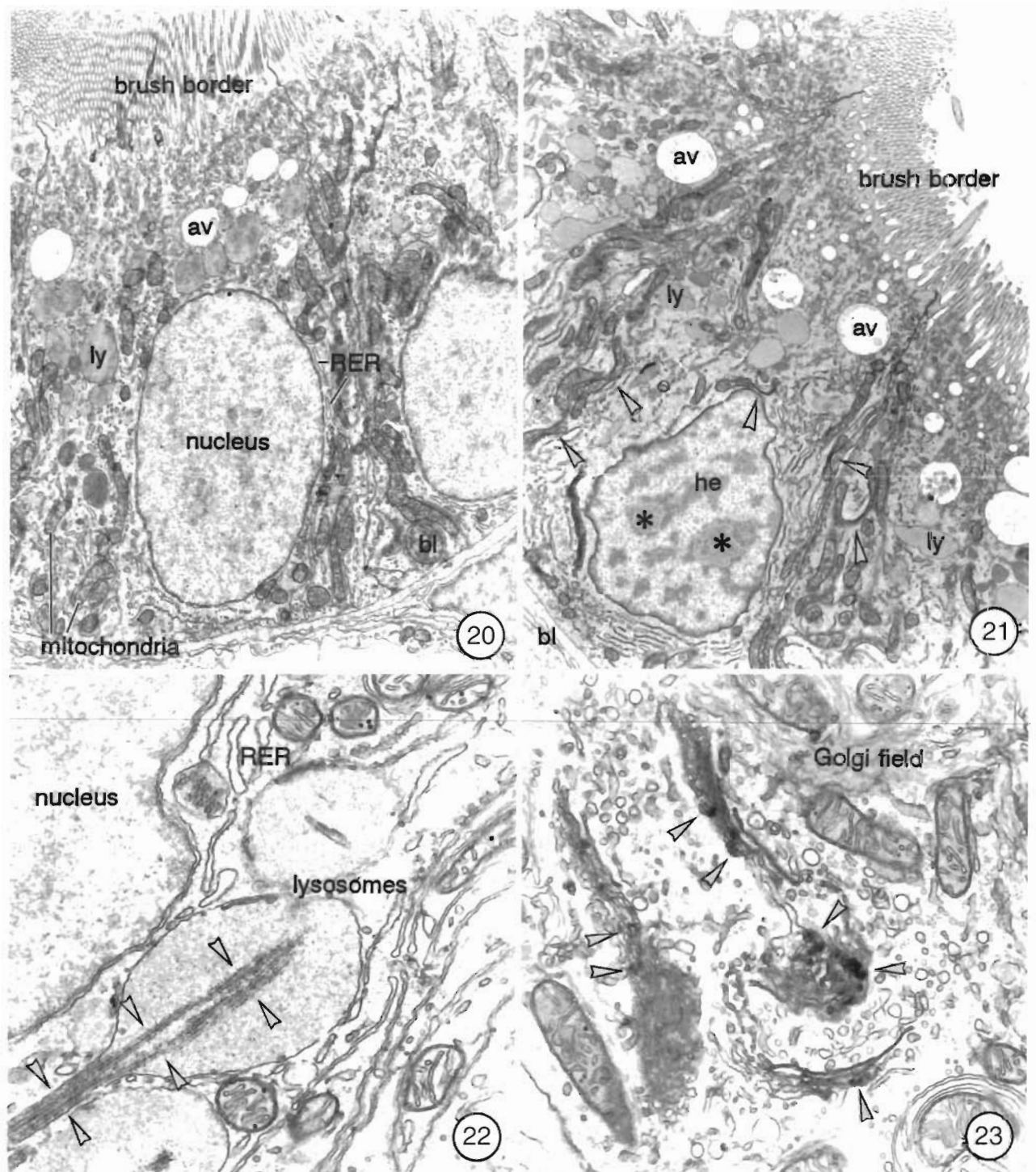
small electron-dense tubular vesicles and electron-lucent endocytotic vesicles form an apical layer of 2 to 3 μm thickness. Electron-lucent vacuoles and numerous lysosomes in the apical half of the cell indicate high endocytotic activity. Golgi fields with 4 to 6 slender cisternae and well-developed RER consisting of slightly dilated elongated cisternae are located next to the nucleus, whereas mitochondria are dispersed in the lower two-thirds of the cell. Peroxisomes are scarce.

Cell height of the proximal segment II (PS II; 16 to 25 μm) is greater, but brush borders are lower (1.9 to 2.3 μm) than in PS I. The nucleus is centrally located (see Fig. 24). An almost 1.5 μm thick layer under the brush border is occupied by numerous small electron-dense tubular vesicles, but no endocytotic activity is observed. Peroxisomes are abundant, and Golgi fields are similar to PS I. The ER system is composed of a tubular meshwork of smooth cisternae and slender RER lamellae located close to the nucleus. PS II cells show a well-developed basal labyrinth. Both PS I and PS II epithelia contain a few ciliated cells.

Distal segments (DS) are marked by diminution of the brush border to few dispersed microvilli. DS are characterized by a narrow lumen and the small diameter of the tubules (see Fig. 31). DS cells protrude irregular portions of cytoplasm into the tubular lumen. The low cuboidal DS cells (diameter 13 to 16 μm) show a centrally to basally located pear-shaped nucleus with



Figs. 18 & 19. *Oncorhynchus mykiss*. In contrast to control fish, where podocytes in renal corpuscles are characterized by spherical nuclei (Fig. 18), the nuclei in rainbow trout exposed to 240 $\mu\text{g l}^{-1}$ linuron (Fig. 19) take a lobulated outline. bl: basal lamina; en: endothelial lining of blood capillary; pe: pedicelles; ps: parietal sheet of Bowman's capsule. Fig. 18: $\times 4900$; Fig. 19: $\times 9400$



Figs. 20 to 23 *Oncorhynchus mykiss*. In comparison to epithelial cells of the proximal segment I in uncontaminated rainbow trout (Fig. 20), fish treated with linuron display more irregular nuclei with an increase in heterochromatin (he) and the number of nucleoli (*), frequent club-shaped mitochondria (arrows, $\geq 120 \mu\text{g l}^{-1}$; Fig. 21), lysosomes with crystalline inclusions ($\geq 30 \mu\text{g l}^{-1}$; Fig. 22 arrowheads), as well as Golgi fields with a high degree of fenestration and vesiculation and myelin-like accumulations of electron dense material between single cisternae ($\geq 30 \mu\text{g l}^{-1}$; Fig. 23: arrowheads). av: apical vacuoles; ly: lysosomes; RER: rough endoplasmic reticulum. Fig. 20: $\times 9900$; Fig. 21: $\times 5200$; Fig. 22: $\times 22400$; Fig. 23: $\times 22300$

little heterochromatin. Golgi fields lie close to the nucleus, and the ER system is composed of small, slender SER and RER scattered throughout the cell. The well-developed basal labyrinth is characterized by numerous mitochondria, which are considerably larger (1 to $2.5\ \mu\text{m}$) than in PS I and PS II (0.4 to $1.5\ \mu\text{m}$), with basal mitochondria being significantly larger than apical ones.

Rainbow trout exposed to linuron

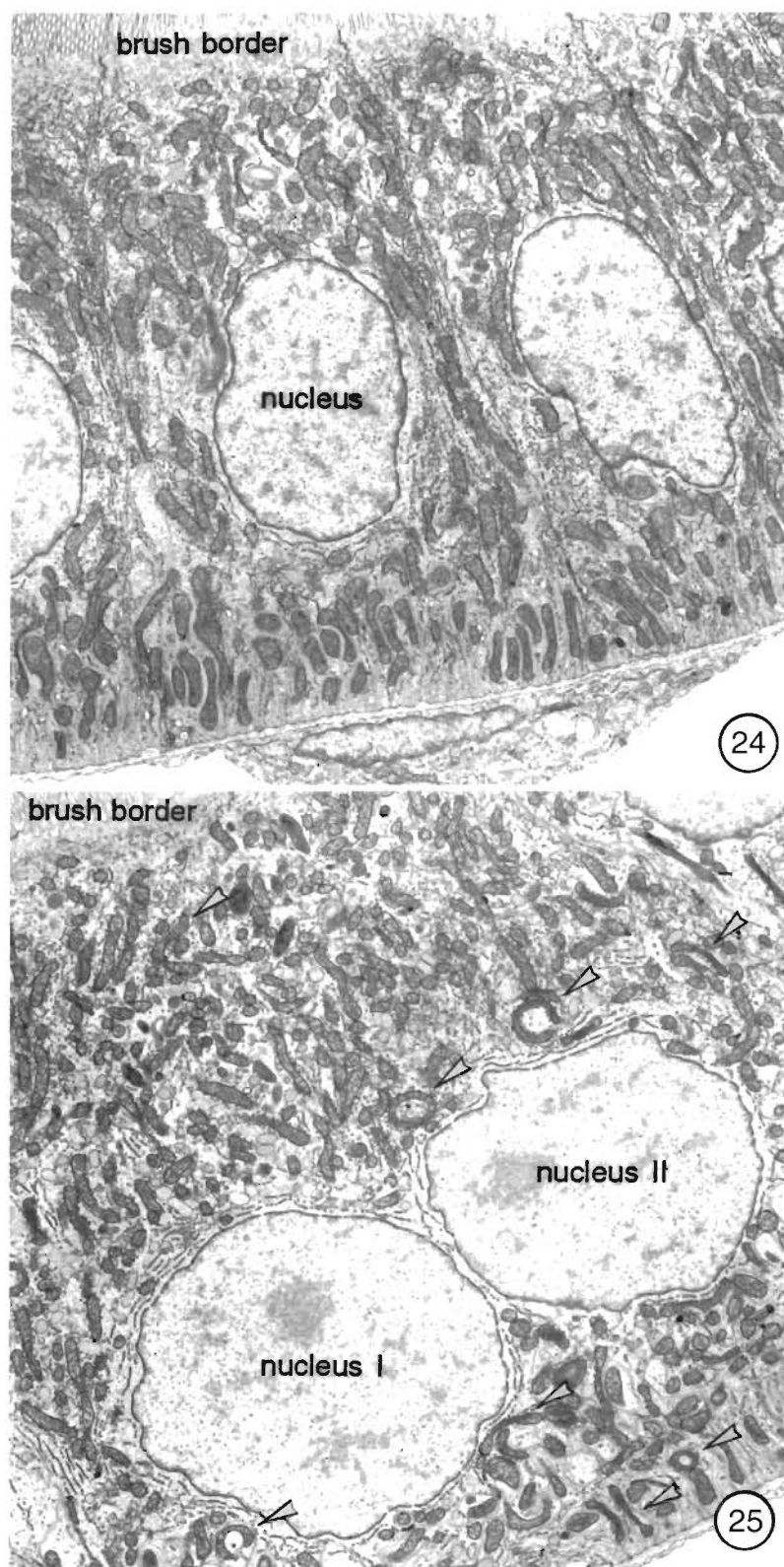
Cytological alterations in different segments of the rainbow trout nephron are summarized in Table 2.

In the renal corpuscle, ultrastructural modifications were restricted to a pronounced lobulation of the podocyte nucleus at $240\ \mu\text{g l}^{-1}$ linuron (Fig. 19).

At $30\ \mu\text{g l}^{-1}$, many PS I nuclei showed irregular outlines and increased amounts of heterochromatin. A few club-shaped mitochondria were observed (Fig. 21). Golgi cisternae displayed an elevated rate of fenestration, and the secretory activity of Golgi fields was increased. Lysosomes proliferated and partly looked fusiform due to long, crystal-like inclusions (Fig. 22).

Changes at $120\ \mu\text{g l}^{-1}$ included further proliferation of club-shaped mitochondria and crystal-bearing lysosomes and myelin-like accumulations of membrane whorls in intercisternal spaces of Golgi fields (Fig. 23). At $240\ \mu\text{g l}^{-1}$, most PS I cells displayed 2 nucleoli as well as a pronounced decrease of mitochondria and lysosomes (Fig. 21), which frequently showed atypical profiles. Mitochondria cristae were often less regularly arranged, and electron-dense myelin-like materials accumulated in the intermembranous space. Likewise, Golgi fields appeared less well organized, and cisternae were highly fenestrated. At $240\ \mu\text{g l}^{-1}$, RER cisternae showed progressive fragmentation and degranulation.

Following exposure to each linuron concentration, single PS I cells displayed more drastic alterations such as increase in nuclear size, reduction of apical microvilli, and formation of



Figs 24 & 25 *Oncorhynchus mykiss*. Whereas epithelial cells of the proximal segment II (PS II) in control rainbow trout are always uninucleated (Fig. 24), PS II cells in fish exposed to $\geq 120\ \mu\text{g l}^{-1}$ linuron may be binucleated and show a conspicuous increase in highly heteromorphic mitochondria (arrowheads), which are less regularly arranged than in controls, as well as lysosomes with crystalline inclusions (Fig. 25). Fig. 24: $\times 4200$, Fig. 25: $\times 5000$.

Table 2. *Oncorhynchus mykiss*. Cytological alterations in different segments of the nephron of rainbow trout after prolonged exposure to sublethal concentrations of linuron. Data are presented as lowest concentration of linuron (in $\mu\text{g l}^{-1}$) at which effect could be observed. *Effect could not be visualized in all specimens examined

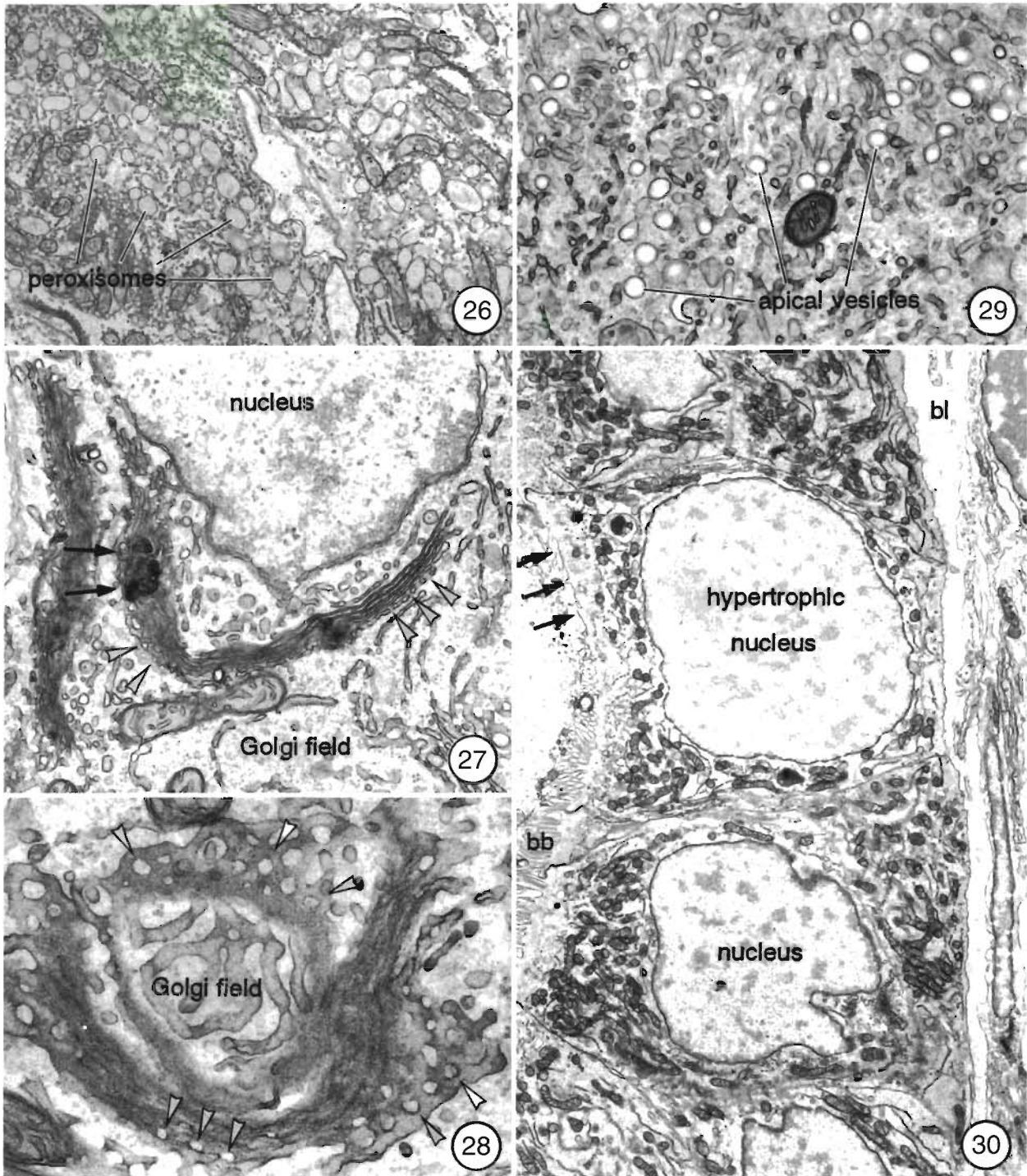
	Renal corpuscle	Proximal segment I	Proximal segment II	Distal segment
General organization				
Invasion of macrophages	–	30	30	30
Nucleus				
Irregular outline	240 (podocytes)	30	30	–
Binucleate cells	–	–	120*	–
Hypertrophy	–	120*	120*	–
Electron-dense accumulations in envelope	–	–	120	–
Mitochondria				
Proliferation of atypical forms	–	30	30	–
Membrane whorls in perimitochondrial space	–	240	30	–
Overall reduction in number	–	240	240	–
Giant mitochondria	–	–	–	30
Crystalline inclusions	–	–	–	30
Longitudinal cristae	–	–	240	30
Peroxisomes				
Proliferation	–	–	30	–
Reduction	–	–	120	–
Formation of clusters	–	–	30	–
Heterogeneity in shape	–	–	120	–
Tail formation	–	–	240	–
Rough endoplasmic reticulum				
Fragmentation and degranulation	–	240	30	–
Golgi fields				
Fenestration	–	30	30	30
Increased secretory activity	–	30	–	–
Membrane whorls between cisternae	–	120*	30*	30*
Electron-lucent areas between cisternae	–	120*	30*	30*
Dilation of cisternae	–	120*	240	30*
Lysosomes				
Proliferation	–	30	30	30
Overall reduction in number	–	240	–	–
Heterogeneity in shape	–	30	30	120
Crystalline inclusions in matrix	–	30	30	240
Induction of autophagosomes	–	–	240	240
Brush border				
Reduction	–	120*	120*	–
Crypt formation	–	120*	120*	–

crypt-like indentations of the apical plasmalemma. The number of macrophages invading PS I progressively increased with linuron concentrations.

At $30 \mu\text{g l}^{-1}$ linuron, PS II revealed nuclear lobulation, proliferation and heterogeneity of lysosomes similar to PS I, and a marked proliferation and cluster formation of peroxisomes (Fig. 26). Golgi cisternae were partially fenestrated and separated by electron-dense myelin-like whorls (Figs. 27 & 28). In addition to alterations similar to PS I, part of the mitochondria were ring-shaped. Mitochondria contained accumulations of myelin-like whorls in the perimitochondrial space or displayed electron-lucent spaces in the matrix. RER cisternae appeared fragmented and degranulated. In many PS II cells, numerous ring-

shaped cisternae either formed envelopes around organelles, e.g. mitochondria, or delineated areas free of organelles. PS II contained more severely altered cells with damaged brush borders and enlarged nuclei than did PS I.

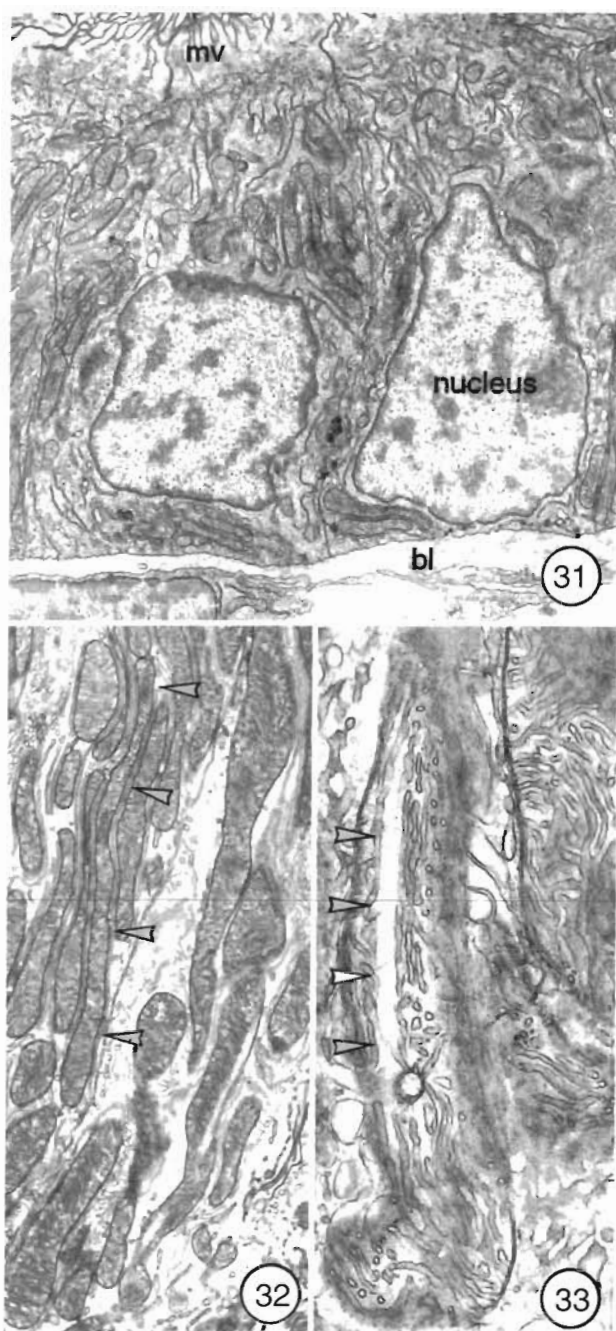
At $120 \mu\text{g l}^{-1}$, peroxisome proliferation was less conspicuous, and peroxisomes were no longer associated in clusters. Similarly, mitochondria appeared less numerous. Atypical lysosomes were increased in size and number. The apices of many cells contained abundant small electron-lucent vesicles (Fig. 29), and elongated or ring-shaped cytoplasmic cisternae were more numerous. Single PS II cells were binucleated (Fig. 25) or displayed accumulations of electron-dense, myelin-like membrane whorls in the perinuclear



Figs. 26 to 30. *Oncorhynchus mykiss*. Ultrastructural modifications in epithelial cells of the PS II include proliferation and formation of peroxisome clusters ($30 \mu\text{g l}^{-1}$ only; Fig. 26), fenestrations (Figs. 27, 28: arrowheads) and accumulation of electron-dense myelin-like material within Golgi fields (Fig. 27: arrows), an increase of apical vesicles (Fig. 29), and occasional hypertrophy of nuclei in combination with atrophy of the brush border (bb; Fig. 30). bl: basal lamina. Fig. 26: $\times 8400$; Fig. 27: $\times 18000$; Fig. 28: $\times 34000$; Fig. 29: $\times 22000$; Fig. 30: $\times 4600$

space. At $240 \mu\text{g l}^{-1}$, peroxisomes and mitochondria in PS II were more decreased, even below control values. Both peroxisomes and mitochondria showed marked

heterogeneity, with peroxisomes often displaying tail-like formations suggesting division, and mitochondria showing slender, elongated profiles with longitudi-



Figs. 31 to 33. *Oncorhynchus mykiss*. In the distal segment, most conspicuous cytological effects by linuron exposure can be found in the mitochondria. If compared to controls (Fig. 31), the longitudinal extension of mitochondria is greatly increased ($\geq 30 \mu\text{g l}^{-1}$, Fig. 32 arrowheads), and mitochondria frequently display crystalline inclusions running in parallel to the longitudinal axis (Fig. 33, arrowheads) as well as longitudinally oriented cristae. bl: basal lamina, mv: microvilli. Fig. 31 $\times 6500$, Fig. 32 $\times 17300$, Fig. 33 $\times 23200$.

nally arranged cristae. The number of lysosomes was apparently increased over controls, yet to a lesser degree than after $\leq 120 \mu\text{g l}^{-1}$. In addition to the

unusual elongated profiles with crystalline inclusions, other lysosomes, probably autophagosomes, contained tubular structures resembling altered Golgi fields. Both small electron-lucent apical vesicles and the elongated cytoplasmic membrane cisternae observed in fish exposed to $120 \mu\text{g l}^{-1}$ were further increased.

PS II sections of fish exposed to $240 \mu\text{g l}^{-1}$ showed severely injured cells and unusual luminal casts (Fig. 30). Nuclei were hypertrophic, irregular, and displayed increased heterochromatin. In addition to giant lysosomes, atrophied brush borders or even complete loss of microvilli were typical of PS II.

DS cells in fish exposed to $30 \mu\text{g l}^{-1}$ were characterized by giant mitochondria (up to $5.6 \mu\text{m}$; Fig. 32), which frequently displayed crystalline inclusions arranged in parallel to the longitudinal axis (Fig. 33), resulting in longitudinal or zig-zag-like arrangement of cristae. In many cells, Golgi fields had dilated cisternae and electron-dense, myelin-like membrane accumulations in the intercisternal spaces. Occasionally, multivesicular bodies were revealed in the cytoplasm. At $120 \mu\text{g l}^{-1}$, giant mitochondria were more numerous, and at $240 \mu\text{g l}^{-1}$ abundant atypical lysosomal profiles with crystal-like inclusions and autophagosomes were common. Between epithelial cells of all segments, there was an apparently dose-dependent infiltration of macrophages.

DISCUSSION

The present study was designed to serve a double purpose: (1) to identify and localize sublethal effects of linuron in liver and kidney epithelial cells of rainbow trout as major organs of biotransformation, and (2) to compare cytological effects in these organs with respect to their nature and the relative sensitivity of liver and kidney. Linuron proved capable of inducing sublethal effects in kidney and liver at $30 \mu\text{g l}^{-1}$, i.e. concentrations about 2 orders of magnitude below the LC_{50} for rainbow trout (Worthing 1987). In both organs, cytopathological alterations were dose-dependent. Since, in the present experiment, linuron of highest analytical grade was used ($\geq 99.96\%$), contamination by tetrachloroazo- and tetrachloroazoxybenzene, which are usually present in at least traces in commercially available linuron (Hill et al. 1981, Di Muccio et al. 1984), can most likely be excluded as causative factors, and cytological alterations in kidney and liver cells may be attributed to linuron or its metabolites.

Potential breakdown products of linuron primarily include chlorinated anilines such as 4-chloroaniline and 3,4-dichloroaniline (Maier-Bode & Hartel 1981, Suzuki & Casida 1981), which have already been studied with regard to ultrastructural alterations in

livers of rainbow trout and zebra fish (Braunbeck et al. 1989, Braunbeck & Segner 1994). A concurrence in effects of linuron and its potential metabolites of approx. 50 % suggests that part of the effects are likely to be due to 4-chloroaniline and 3,4-dichloroaniline. These common effects appear indicative of specific physiological processes and may, thus, give a hint to the possible mode of action of linuron.

The stimulation of nuclear division, e.g. in conjunction with signs of reorganization of nuclear and nucleolar components, indicates that the nucleus represents one major site of toxic action. Since one primary effect of linuron in plants is also interaction with chromosomes, mitosis and cell division (Maier-Bode & Hartel 1981), nuclear changes might well be related to the suspected carcinogenic potential of linuron (Sabbioni & Neumann 1990) and/or the carcinogenic risk of its parent and breakdown products. In fact, the carcinogenicity of linuron might well result from hydrolytic breakdown to aromatic chlorinated anilines, which, by N-hydroxylation, can be easily transformed to nitrosoarene compounds via nitroso compounds and hydroxylamine in rainbow trout (Dady et al. 1991).

In rainbow trout, fractionation, vesiculation and dilation of RER cisternae are frequently found in parallel to SER proliferation. This suite of alterations has been documented in mammals after exposure to phenobarbital, polychlorinated biphenyls and the polycyclic aromatic hydrocarbon 3-methylcholanthrene and is generally regarded indicative of the induction of detoxification processes both in mammals (for reviews see Phillips et al. 1987 and Ghadially 1988) and fish (Hinton et al. 1978, Lipsky et al. 1978, Schoor & Couch 1979, Hawkes 1980, Rojik et al. 1983, Braunbeck et al. 1989, 1990a, b, 1992a, b, Braunbeck & Völkl 1991).

Quantitative alterations and increased morphological heterogeneity of mitochondria and peroxisomes are further common features of exposure to linuron, 4-chloroaniline and 3,4-dichloroaniline (Braunbeck et al. 1990b, Braunbeck & Segner unpubl.). Mitochondrial heterogeneity most likely represents the morphologic expression of physiologic acclimatization processes in response to growing oxygen requirements (Ghadially 1988). Possibly, mitochondrial proliferation may be an adaptive process compensating for the decoupling activity of linuron described in isolated rat mitochondria (Abo-Khatwa & Hollingworth 1974). Processes leading to peroxisome proliferation in fish liver have not yet been studied in detail. Based on results from studies in mammals, however, one reason might be formation of peroxides (Phillips et al. 1987). In fact, of a range of 12 organic reference toxicants and pesticides tested so far in our laboratory with respect to ultrastructural changes in the livers of zebrafish, rainbow trout, medaka, carp *Cyprinus carpio*, and various

ornamental fish species, lindane (Braunbeck et al. 1990a), 3,4-dichloroaniline (Braunbeck & Segner 1994), and linuron were the only compounds inducing true peroxisome proliferations.

Hepatic lipid accumulation within RER membranes, originally described as 'steatosis' or 'liposomes' by Baglio & Farber (1965), may result from either a blockade in VLDL secretion or an imbalance between protein and lipid components in lipoprotein metabolism. These alterations have repeatedly been reported in fish liver under adverse conditions (Deplano et al. 1989, Braunbeck et al. 1990a, Segner & Witt 1990, Braunbeck & Segner 1993). Since, despite the considerable increase in hepatocellular lipid deposits, linuron exposure results more in a stimulation than in a depression of Golgi activity, and since there is a decrease in RER, disturbances in protein synthesis appear more likely as a reason for hepatic steatosis than a blockade in lipoprotein secretion. In fact, the degradation of large amounts of membrane-like materials within lysosomal profiles ('phospholipidosis'; Phillips et al. 1987) suggests the immediate decomposition of membrane structures containing excess phospholipid components. Thus, in addition to the nucleus, intracellular membrane complexes involved in both protein and lipid metabolism seem to be major targets of linuron toxicity.

Since immigration of macrophages and removal of damaged cell components ($\geq 30 \mu\text{g l}^{-1}$) as well as necrotic hepatocytes ($\geq 120 \mu\text{g l}^{-1}$) per se represent adaptive rather than degenerative features, there is an obvious shift in the reaction of rainbow trout to linuron between 30 and $120 \mu\text{g l}^{-1}$ in terms of a transition from adaptation to degeneration. Such a biphasic reaction to linuron is not only also evident in the proximal segment II (PS II) of the kidney with regard to proliferation and aggregation of peroxisomes at $30 \mu\text{g l}^{-1}$ and decrease and dispersal at $\geq 120 \mu\text{g l}^{-1}$, but also in phagocytic activity of leucocytes (Falk et al. 1990). Since the LC_{50} of linuron for rainbow trout is given as 5 mg l^{-1} (Worthing 1987), this transition to degeneration at the cellular level by far precedes detrimental effects at the organismic level.

With regard to the relative sensitivity of organs investigated, the kidney proved to be at least as sensitive to linuron as did the liver (cf. e.g. Trump & Bulger 1968a, b). The present investigation revealed a clear selectivity of cytological effects for specific zones of the nephron. Although podocytes and, to a lesser extent, cells of other tubular segments also displayed distinct cytological modifications, maximum effect by linuron exposure could be recorded in PS II. Thus, in agreement with findings by Rojik et al. (1983), Benedeczky et al. (1986), and Reimschuessel et al. (1989), the tubular portion of the fish nephron apparently reacts with higher sensitivity than the renal corpuscle.

Although fish liver may comprise as many as 20 different cell types, in most species more than 90% of the volume is accounted for by hepatocytes (Hampton et al. 1989). Although exposure to xenobiotics usually results in an increase of heterogeneity between single hepatocytes (Braunbeck 1994), the present study revealed that the reaction of liver cells appeared more homogeneous than that of epithelial cells in different zones of the nephron. This might be due to the fact that the number of hepatocytes in mitosis (as an indicator of hepatocellular turnover rate) is much lower in fish than in mammals, i.e. that all hepatocytes were most likely exposed to linuron for the same period of time. In contrast, as a consequence of constant renewal of both renal tubules and epithelial cells within the tubules (Hentschel & Elger 1987), control nephronic epithelia already display higher heterogeneity than control livers. This underlying heterogeneity apparently results in even higher heterogeneity in nephronic cellular response to xenobiotics. In carp exposed to paraquat, ultracid and CuSO_4 , e.g., the level of damage in kidney epithelial cells was also highly heterogeneous, i.e. relatively intact cells were frequently found adjacent to severely altered cells (Benedeczky et al. 1986). Similar observations could be made in the kidney of rainbow trout exposed to linuron, with differences in cellular modifications in PS II being so prominent that PS II cells could be classified into 2 distinct reaction types: reaction type I was characterized by dose-dependent biphasic peroxisome reactions, occurrence of lysosomes with crystalline inclusions, dense brush border, and conspicuous overall decrease of organelles, whereas reaction type II could be identified by degenerative features such as hypertrophic nuclei, highly irregular arrangement of the brush border, and absence of peroxisome proliferation. As a consequence of this heterogeneity, the thorough assessment of toxicant-induced kidney changes requires the inspection of more sections and is, thus, more time- and labour-consuming than corresponding liver studies. On the other hand, the differential reaction of different tubular segments might again give clues as to the mechanisms of the toxicants investigated. The high number of peroxisomes in combination with increased levels of sensitivity observed in PS II, for example, might indicate that either biomagnification of toxicants reaches its maximum in this tubular portion or, as in mammals (Zaar 1992), biotransformation rates in fish kidney are highest in PS II. Either of these hypotheses can be supported by the fact that the interstitial tissues between renal tubules displayed considerable injury related to linuron exposure (data not shown), thus indicating that linuron or its metabolites most likely reach PS II cells via blood vessels and are excreted by active secretion in the renal tubule rather than by direct filtration in the

glomerulus. Such a mechanism of non-glomerular excretion, e.g., has been demonstrated for the herbicide 2,4-dichlorophenoxyacetic acid in isolated flounder tubules (Pritchard & Bend 1984).

LITERATURE CITED

- Abo-Khatwa N, Hollingworth RM (1974) Pesticidal chemicals affecting some energy-link functions of rat liver mitochondria *in vitro*. *Bull environ Contam Toxicol* 12:446–434
- Arnold H, Braunbeck T (1994) Disulfoton as a major toxicant in the Rhine chemical spill at Basel in November 1986: acute and chronic studies with eel and rainbow trout. In: Proceedings of the XVII EIFAC Symposium of sublethal and chronic effects of pollutants on freshwater fish. In press
- Baglio CM, Farber E (1965) Reversal by adenine of the ethionine-induced lipid-accumulation in the endoplasmic reticulum of the rat liver. *J Cell Biol* 27:591–601
- Benedeczky I, Nemcsok J, Halasy K (1986) Electron microscopic analysis of the cytopathological effect of pesticides in the liver, kidney and gill tissues of carp. *Acta Biol Szeged* 32:69–91
- Berlin JD, Dean JM (1967) Temperature-induced alterations in hepatocyte structure of rainbow trout. *J exp Zool* 164:117–132
- Braunbeck T (1993) Cytological alterations in isolated hepatocytes from rainbow trout (*Oncorhynchus mykiss*) exposed to 4-chloroaniline. *Aquat Toxicol* 25:83–110
- Braunbeck T (1994) Detection of environmentally relevant concentrations of toxic organic compounds using histological and cytological parameters: substance-specificity in the reaction of rainbow trout liver? In: Proceedings of the XVII EIFAC Symposium on sublethal and chronic toxic effects of pollutants on freshwater fish. In press
- Braunbeck T, Burkhardt-Holm P, Gorge G, Nagel R, Negele RD, Storch V (1992a) Regenbogenforelle und Zebrafärbung, zwei Modelle für verlängerte Toxizitätstests: relative Empfindlichkeit, Art- und Organspezifität in der cytopathologischen Reaktion von Leber und Darm auf Atrazin. *Schriftenr. Ver. Wasser-, Boden-, Lufthyg.* 89: 109–145
- Braunbeck T, Gorge G, Storch V, Nagel R (1990a) Hepatic steatosis in zebra fish (*Brachydanio rerio*) induced by long-term exposure to γ -hexachlorocyclohexane. *Ecotox Environ Safety* 19:355–374
- Braunbeck T, Storch V, Bresch H (1990b) Species-specific reaction of liver ultrastructure of zebra fish (*Brachydanio rerio*) and trout (*Salmo gairdneri*) after prolonged exposure to 4-chloroaniline. *Arch environ Contam Toxicol* 19:405–418
- Braunbeck T, Storch V, Nagel R (1989) Sex-specific reaction of liver ultrastructure in zebra fish (*Brachydanio rerio*) after prolonged sublethal exposure to 4-nitrophenol. *Aquat Toxicol* 14:185–202
- Braunbeck T, Teh SJ, Lester SM, Hinton DE (1992b) Ultrastructural alterations in hepatocytes of medaka (*Oryzias latipes*) exposed to diethylnitrosamine. *Toxicol Pathol* 20:179–196
- Braunbeck T, Völkl A (1991) Induction of biotransformation in the liver of eel (*Anguilla anguilla* L.) by sublethal exposure to dinitro-*o*-cresol: an ultrastructural and biochemical study. *Ecotox Environ Safety* 21:109–127
- Braunbeck T, Völkl A (1993) Toxicant-induced cytological alterations in fish liver as biomarkers of environmental

- pollution? A case-study on hepatocellular effects of dinitro-*o*-cresol in golden ide (*Leuciscus idus melanotus*). In: Braunbeck T, Hanke W, Segner H (eds) Fish in ecotoxicology and ecophysiology. Verlag Chemie, Weinheim, p 55–80
- Chapman GB (1981) Ultrastructure of the liver of the fingerling rainbow trout, *Salmo gairdneri*. J Fish Biol 18: 553–567
- Dady JM, Bradbury SP, Hoffman AD, Voit MM, Olson DL (1991) Hepatic microsomal N-hydroxylation of aniline and 4-chloroaniline by rainbow trout (*Oncorhynchus mykiss*). Xenobiotica 21:1605–1620
- Deplano M, Connes R, Diaz JP, Paris J (1989) Intestinal steatosis in the farm-reared sea bass, *Dicentrarchus labrax*. Dis aquat Org 6:121–130
- Di Muccio A, Camoni I, Dommarco R (1984) 3,3',4,4'-Tetrachloroazobenzene and 3,3',4,4'-tetrachloroazoxybenzene in technical grade herbicides: propanil, diuron, linuron and neburon. Ecotox Environ Safety 8:511–515
- Falk HF, Negele R-D, Goerlich R (1990) Phagocytosis activity as an in vitro test for the effects of chronic exposure of rainbow trout to Linuron, a herbicide. J appl Ichthyol 6: 231–236
- Fischer-Scherl T, Veese A, Hoffmann RW, Kuhnhauser C, Negele RD, Ewringmann T (1991) Morphological effects of acute and chronic atrazine exposure in rainbow trout (*Oncorhynchus mykiss*). Arch environ Contam Toxicol 20:454–461
- Fishbein L (1972) Pesticidal, industrial, food additive, and drug mutagens. In: Sutton HE, Harris MI (eds) Mutagenic effects of environmental contaminants. Academic Press, New York, p 129–170
- Ghadially FN (1988) Ultrastructural pathology of the cell and matrix, Vols I + II. Butterworths, London
- Greve PA, Wegman RCC (1975) Bestimmung und Vorkommen von aromatischen Aminen und ihrer Derivate in niederländischen Oberflächengewässern. Schriftenr Ver Wasser-, Boden-, Lufthyg 46:325
- Hacking MA, Budd J, Hodson K (1978) The ultrastructure of the liver of the rainbow trout: normal structure and modifications after chronic administration of a polychlorinated biphenyl Aroclor 1254. Can J Zool 56:477–491
- Hampton JA, Lantz RC, Goldblatt PJ, Laurén DJ, Hinton DE (1988) Functional units in rainbow trout (*Salmo gairdneri*, Richardson) liver: II. The biliary system. Anat Rec 221: 619–634
- Hampton JA, Lantz RC, Hinton DE (1989) Functional units in rainbow trout (*Salmo gairdneri*, Richardson) liver: III. Morphometric analysis of parenchyma, stroma, and component cell types. Am J Anat 185:58–73
- Hampton JA, McCuskey PA, McCuskey RS, Hinton DE (1985) Functional units in rainbow trout (*Salmo gairdneri*) liver. I. Arrangement and histochemical properties of hepatocytes. Anat Rec 213:166–175
- Hawkes JW (1980) The effects of xenobiotics on fish tissues: morphological studies. Fed Proc 39:3230–3236
- Hentschel H, Elger M (1987) The distal nephron in the kidney of fishes. Adv Anat Embryol Cell Biol 106:1–151
- Hentschel H, Finkenstädt H (1980) Perfusion fixation and alcian-blue PAS staining in histology and histopathology of teleost kidney. J Fish Dis 3:473–479
- Herzel F, Schmidt G (1977) Pflanzenschutzmittel-Spuren in Umweltproben. Bundesgesundheitsblatt 20:221–223
- Hill RH, Rollen ZJ, Kimbrough RD, Groce DF, Needham LL (1981) Tetrachloroazobenzene in 3,4-dichloroaniline and its herbicidal derivatives: propanil, diuron, linuron, and neburon. Arch environ Health 36:11–14
- Hinton DE, Klaunig JE, Lipsky MM. (1978) PCB-induced alterations in teleost liver: a model for environmental disease in fish. Mar Fish Rev 40:47–50
- Hodge HC, Downs WL, Smith DW, Maynard EA, Clayton JW, Pease HL (1968) Oral toxicity of linuron [3(3,4-dichlorophenyl)-1-methoxy-1-methylurea] in rats and dogs. Food Cosmet Toxicol 6:171–183
- Hsia MTS, Bairstow FVZ, Shin LCT, Pounds JG, Allen JR (1977) 3,4,3',4'-Tetrachloroazobenzene: a potential environmental toxicant. Res Commun Chem Pathol Pharmacol 17:225–236
- Johnson RD, Teitge YE (1991) Carcinogenic sensitivity of the medaka to aromatic amines. Abstracts of the 30th annual Society of Toxicology meeting. Toxicologist 11:331
- Karnovsky MJ (1971) Use of ferrocyanide-reduced osmium tetroxide in electron microscopy. J Cell Biol 51:146A
- Kempson-Jones GF, Hanel RJ (1979) Kinetics of linuron and metribuzin degradation in soil. Pest Sci 10:449–454
- Knauf W, Schulze EF (1972) Langzeiteinfluß subletaler Herbiziddosen auf einige Vertreter der Wasserfauna und -flora am Beispiel Linuron und Monolinuron. Schriftenr Ver Wasser-, Boden-, Lufthyg 37:231
- Lewalter J, Korallus U (1986) Erythrocyte protein conjugates as a principle of biological monitoring for pesticides. Tox Letters 33:153–165
- Lipsky MM, Klaunig JE, Hinton DE (1978) Comparison of acute response to polychlorinated biphenyl in liver of rat and channel catfish: a biochemical and morphological study. J Toxicol environ Health 4:107–121
- Maier-Bode H, Hartel K (1981) Linuron and monolinuron. Residue Rev 77:1–364
- Malle KG (1984) Die Bedeutung der 128 Stoffe der EG-Liste für den Gewässerschutz. Z Wasser Abw Forsch 17:75–81
- Marshall TC, Dorough HW, Swim HC (1976) Screening of pesticides for mutagenic potential using *Salmonella typhimurium* mutants. J Agric Food Chem 24:560–563
- Phillips MJ, Poucell S, Patterson J, Valencia P (1987) The liver — an atlas and text of ultrastructural pathology. Raven Press, New York
- Pritchard JB, Bend JR (1984) Mechanisms controlling the renal excretion of xenobiotics in fish: effects of chemical structure. Drug Metab. Rev. 15:655–671
- Reimschuessel R, Bennett RO, May EB, Lipsky MM (1989) Renal histopathological changes in the goldfish (*Carassius auratus*) after sublethal exposure to hexachlorobutadiene. Aquat Toxicol 15:169–180
- Reynolds ES (1963) The use of lead citrate at high pH as an electron-opaque stain in electron microscopy. J Cell Biol 17:208–212
- Richardson KC, Jarett L, Finke EH (1960) Embedding in epoxy resins for ultrathin sectioning in electron microscopy. Stain Technol 35:313–323
- Rojik I, Nemcsók J, Boross L (1983) Morphological and biochemical studies on liver, kidney and gill of fishes affected by pesticides. Acta Biol Hung 34:81–92
- Roloff BD, Belluck DA, Meisner LF (1992) Cytogenetic studies of herbicide interactions *in vitro* and *in vivo* using atrazine and linuron. Arch environ Contam Toxicol 22:267–271
- Sabbioni G, Neumann HS (1990) Biomonitoring of arylamines: haemoglobin adducts of urea and carbamate pesticides. Carcinogenesis 11:111–115
- Scarpelli DG, Greider MH, Frajola WJ. (1963) Observations on hepatic cell hyperplasia, adenoma and hepatoma of rainbow trout (*Salmo gairdneri*). Cancer Res 23:848–856
- Scharankel KR, Hsia MTS, Pounds JC (1980) Hepatocellular pathotoxicology of 3,3',4,4'-tetrachloroazobenzene and 3,3',4,4'-tetrachloroazoxybenzene. Res Commun Chem

- Pathol Pharmacol 28:527–540
- Scharankel KR, Kreamer BL, Hsia MTS (1982) Embryotoxicity of 3,3',4,4'-tetrachloroazobenzene and 3,3',4,4'-tetrachloroazoxybenzene in the chick embryo. Arch environ Contam Toxicol 11:195–202
- Schoor WP, Couch JA (1979) Correlation of mixed-function oxidase activity with ultrastructural changes in the liver of a marine fish. Cancer Biochem Biophys 4:95–103
- Segner H, Witt U (1990) Weaning experiment with turbot (*Scophthalmus maximus*): electron microscopic study of the liver. Mar Biol 105:353–361
- Singh I (1964) A modification of the Masson-Hamperl method for staining of argentaffin cells. Anat Anz 115:81–82
- Spurr AR (1969) A low viscosity embedding medium for electron microscopy. J Ultrastr Res 26:31–43
- Sundström G, Jansson B, Renberg L (1978) Determination of the toxic impurities 3,3',4,4'-tetrachloroazobenzene in commercial diuron, linuron and 3,4-dichloroaniline samples. Chemosphere 12:973–979
- Suzuki T, Casida JE (1981) Metabolites of diuron, linuron, and methazole formed by liver microsomal enzymes and spinach plants. J Agric Food Chem 29:1027–1033
- Tooby TE, Hursey PA, Alabaster JS (1975) The acute toxicity of 102 pesticides and miscellaneous substances to fish. Chemistry and Industry 21 June, p 523–526
- Trump BF, Bulger RE (1968a) Studies of cellular injury in isolated flounder tubules. III. Light microscopical and functional changes due to cyanide. Lab Invest 18:721–730
- Trump BF, Bulger RE (1968b) Studies of cellular injury in isolated flounder tubules. IV. Electron-microscopic observations of changes during the phase of altered homeostasis in tubules treated with cyanide. Lab Invest 18:731–739
- Wester PW, Canton JH (1986) Histopathological study of *Oryzias latipes* (medaka) after long-term β -hexachloro-cyclohexane exposure. Aquat Toxicol 9:21–45
- Worthing CR (1987) The pesticide manual, 8th edn. The British Crop Protection Council, Thornton Heath
- Yasutake WT, Wales JH (1983) Microscopic anatomy of salmonids: an atlas. United States Department of the Interior, Fish and Wildlife Service, Resource Publ. 150, Washington, DC
- Zaar K (1992) Structure and function of peroxisomes in the mammalian kidney. Eur J Cell Biol 59:233–254
- Zahn T, Braunbeck T (1993) Isolated fish hepatocytes as a tool in aquatic toxicology: sublethal effects of dinitro-*o*-cresol and 2,4-dinitrophenol. Sci tot Environ Suppl 1993: 721–734
- Zahn T, Hauck C, Braunbeck T (1993) Cytological alterations in fish fibrocytic R1 cells as an alternative test system for the detection of sublethal effects of environmental pollutants: a case-study with 4-chloroaniline. In: Braunbeck T, Hanke W, Segner H (eds) Fish in ecotoxicology and eco-physiology. Verlag Chemie, Weinheim, p. 103–126
- Zahnow EB, Riggelman JD (1980) Search for linuron residues in tributaries of the Chesapeake Bay. J Agric Food 28: 974–978

Responsible Subject Editor: D. E. Hinton, Davis, California, USA

Manuscript first received: January 8, 1994

Revised version accepted: August 10, 1994